Progress In Electromagnetics Research C, Vol. 112, 35–44, 2021

A New Reflectionless Filter Composed of Discharging Circuit

Aixia Yuan[1, 2], Shaojun Fang[1, *], Ying Wang[2], Yulin Feng[1], and Tielin Zhang[1]

Abstract—A new reflectionless filter with a discharging circuit is presented. Under the premise of keeping the original filter unchanged, a discharging circuit is added. The relationship between the passband and stopband of the discharging circuit and the original filter is similar to the duality of the circuit. Without affecting the performance of the original filter, the reflected energy of the original filter is discharged to the ground through discharging circuit, so as to achieve no reflection of the filter, avoiding the interference to the input. Analytical design equations are provided so that the reflectionless filter can be designed. According to this design method, the reflectionless dual-band bandpass filter is designed and fabricated. Simulation and measurement results are in agreement. It has good reflectionless performance. The feasibility of the design method is verified.

1. INTRODUCTION

The reflection of rejected band signals is harmful for some filter circuits and adversely affects their performance in some applications such as mixers and high gain amplifiers. Therefore, in circuits, It is better to discharge the out of band frequencies to the ground instead of reflecting them to the input. On this basis, reflectionless filters could be useful and necessary.

To eliminate the reflected signals present in the filter stopband, a lot of research has been done [1–6]. Two approaches have been introduced for lumped parameter element reflectionless filters. The first approach presents a symmetric circuit [1–3]. The disadvantage of the first approach is that the reflectionless filter can only be used as a whole and cannot be split. The second approach presents an impedance matching circuit [4]. In [4], while the reflectionless design is added, the component value of the original filter will change, so it is unable to achieve no reflection directly on the basis of the original circuit. The new design method of the reflectionless filter proposed in this paper still keeps the structure and component value of the original filter unchanged and only adds the discharging circuit on the basis of the original circuit. This design can be used to directly design the reflectionless filter or to upgrade the original filter without reflectionless function. In the case of upgrading the original filter to no reflection, there is no need to change the original product or design, thus saving time and cost.

Wireless communication systems are moving towards multifunctional and multimodal, which requires the ability to select two or more operating frequency bands of signals simultaneously. At the same time, different dual-band bandpass filters with excellent performance and compact size are in tremendous demand with the rapid growth of various wireless communication systems. Recently, many scholars have designed dual-band bandpass filters [7–19] and reflectionless dual-band bandpass filters (RDBPFs) [20–24]. Thus, this work presents a new reflectionless dual-band bandpass filter based on this method proposed in this paper.

This paper is organized as follows. In the second section, the basic bandpass is taken as examples to calculate and deduce the equation, and the structure and component values of the discharging circuit

Received 14 March 2021, Accepted 9 April 2021, Scheduled 16 April 2021

* Corresponding author: Shao-Jun Fang (fangshj@dlmu.edu.cn).

[1] Antenna and Microwave Institute, Dalian Maritime University, Dalian 116026, China. [2] School of Information Science and Engineering, Dalian Polytechnic University, Dalian 116034, China.

are deduced. The correctness of the theory is verified by the simulation of the discharging circuit and the whole circuit. In the third section, a dual-band bandpass filter is designed, manufactured, and measured. In the fourth section, a reflectionless dual-band bandpass filter is implemented according to this design method. It is simulated and fabricated. The simulation and measurement results are almost the same, and the feasibility of the design is verified.

2. A NEW METHOD FOR DESIGNING REFLECTIONLESS FILTER

The structure of a new reflectionless filter is shown in Fig. 1. Z_1 and Z_2 are the impedance of the original filter and discharging circuit.

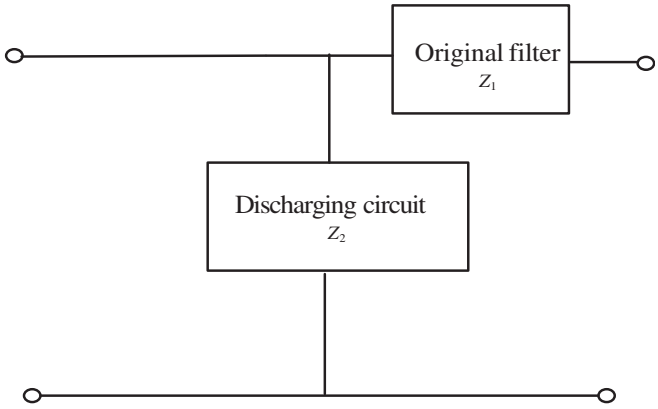

Figure 1. Reflectionless filter diagram.

S-parameter and $ABCD$ parameter can describe a two-port network. Each parameter has a certain relationship with S_{11}, which can be expressed by the following Equation (1).

$$S_{11} = \frac{A + \dfrac{B}{Z_0} - CZ_0 - D}{A + \dfrac{B}{Z_0} + CZ_0 + D} \tag{1}$$

where Z_0 denotes the characteristic impedance of the reflectionless filter.

The $ABCD$ matrix of the reflectionless filter is in Equation (2)

$$\begin{bmatrix} A & B \\ C & D \end{bmatrix} = \begin{bmatrix} 1 & Z_1 \\ \dfrac{1}{Z_2} & 1 + \dfrac{Z_1}{Z_2} \end{bmatrix} \tag{2}$$

If the circuit is reflectionless, it is required that $S_{11} = 0$. From Equation (1), Equation (3) is obtained.

$$A + \frac{B}{Z_0} = CZ_0 + D \tag{3}$$

Given Z_1 a known filter circuit, substituting the values in Eq. (2) into Eq. (3), Equation (4) is obtained. If Equation (4) is satisfied between Z_1 and Z_2, the filter of this structure can achieve no reflection. The circuit with an impedance of Z_2 is called discharging circuit. When the original filter with an impedance of Z_1 is designed, the discharging circuit can be obtained according to Z_2. Then, a new reflectionless filter is obtained.

$$Z_2 = Z_0 + \frac{Z_0^2}{Z_1} \tag{4}$$

In order to realize no reflection of the band-pass filter composed of the capacitance C_1 and inductance L_1 as shown in Fig. 2, it is necessary to add a discharging circuit with an impedance value of Z_2 to realize a simple reflectionless band-pass filter.

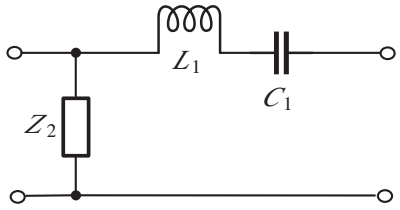

Figure 2. Reflectionless bandpass filter.

In Fig. 2, the impedance of the original filter is Equation (5). When there is no reflection, the impedance of the discharging circuit is Equation (6).

$$Z_1 = SL_1 + \frac{1}{SC_1} \tag{5}$$

$$Z_2 = Z_0 + \frac{Z_0^2}{Z_1} = Z_0 + \frac{Z_0^2}{SL_1 + \frac{1}{SC_1}} = Z_0 + \frac{1}{S\frac{L_1}{Z_0^2} + \frac{1}{SC_1 Z_0^2}} \tag{6}$$

Equation (7) is obtained. Z_2 is composed of a resistor R with resistance Z_0 and a parallel circuit with capacitance C_2 and inductance L_2, as shown in Fig. 3.

$$C_2 = \frac{L_1}{Z_0^2}, \quad L_2 = C_1 Z_0^2, \quad R = Z_0 \tag{7}$$

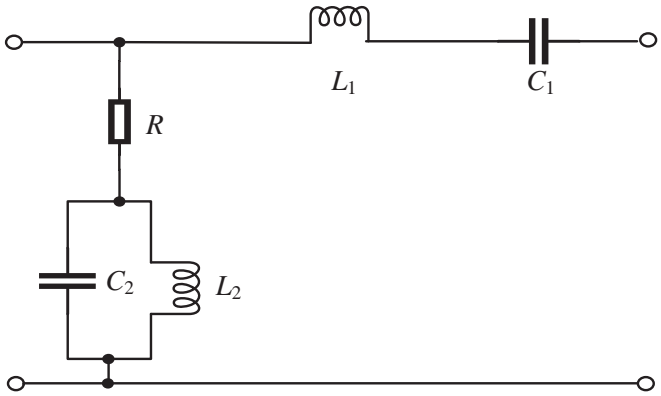

Figure 3. Detailed reflectionless bandpass filter.

When the capacitance and inductance are $C_1 = 24\,\text{pF}$, $C_2 = 108\,\text{pF}$, $L_1 = 270\,\text{nH}$, $L_2 = 60\,\text{nH}$ and resistance is $R = Z_0 = 50\,\Omega$, the simulation is shown in Fig. 4. The purple line indicates S_{21} of the reflectionless filter. The blue line indicates S_{21} of the discharging circuit. S_{11} of the proposed reflectionless filter is not shown in Fig. 4 since it is $-\infty\,\text{dB}$ over the entire frequency. It can be seen from Fig. 4 that the condition of no reflection is satisfied.

It can be seen in Fig. 4(a) that the discharging circuit and original filter are similar to duality. The passband of the discharging circuit corresponds to the stopband of the original filter, and the stopband of the discharging circuit corresponds to the passband of the original filter.

$S_{11} = 0$ is only realized under theory simulation conditions. In practice, due to the error of capacitance and inductance, the reflectionless value cannot be zero.

The quality factor Q value affects the selectivity and bandwidth of the filter. According to the circuit in Fig. 3, Q values are different when capacitance and inductance are different. Simulation results are shown in Fig. 4(b).

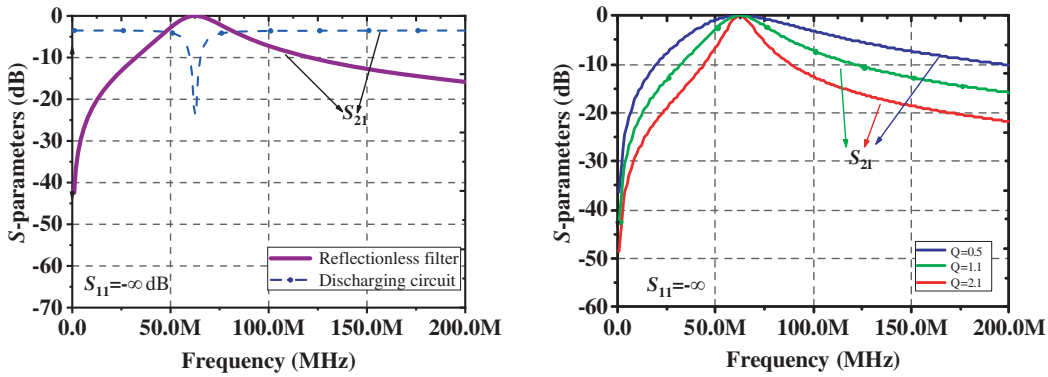

Figure 4. Theoretical simulation: (a) Reflectionless bandpass filter; (b) Reflectionless filter of different Q values.

3. THE DESIGN OF DUAL-BAND BANDPASS FILTER

The schematic diagram dual-band bandpass filter (DBPF) is composed of series and parallel resonance circuits using inductor and capacitor, as shown in Fig. 5. When the values of capacitance and inductance change, the central frequency of the filter is variable, and the circuit structure remains unchanged.

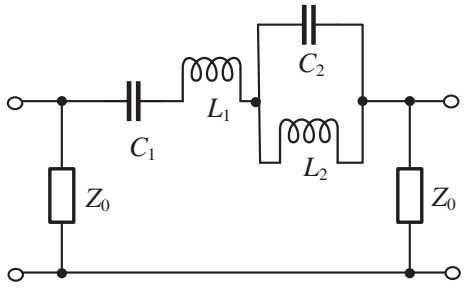

Figure 5. Dual-band bandpass filter.

L_1 and L_2 represent inductance; C_1 and C_2 represent capacitance; Z_0 represents the input and output characteristic impedance.

The transmission function of the filter is in Equation (8).

$$H(j\omega) = \frac{Z_0}{(j\omega L_1) + \left(\frac{1}{j\omega C_1}\right) + \frac{\left(\frac{j\omega L_2}{jwC_2}\right)}{(j\omega L_2) + \left(\frac{1}{j\omega C_2}\right)} + Z_0} \tag{8}$$

where ω represents the angular frequency.

The centre frequencies vary with the capacitance and inductance while the circuit structure remains unchanged. The theory simulation of dual-band band-pass characteristics is shown in Fig. 6. Its centre frequencies are 39 MHz and 101 MHz, respectively, when $L_1 = L_2 = 270\,\text{nH}$, $C_1 = C_2 = 24\,\text{pF}$, $Z_0 = 50\,\Omega$ as shown in state1 of Fig. 6. The first passband is 30–46 MHz with a 3 dB-bandwidth of 16 MHz. The second passband is 85–129 MHz with a 3 dB-bandwidth of 44 MHz. If the inductance and impedance remain unchanged, the capacitance values are taken as $C_1 = C_2 = 10\,\text{pF}$ or $C_1 = C_2 = 5\,\text{pF}$, and the simulation results are shown in state2 and state3 of Fig. 6. Without a reflectionless circuit, the reflection is very large as shown in Fig. 6. The lumped elements values of the three dual-band bandpass filters with different center frequencies are shown in Table 1.

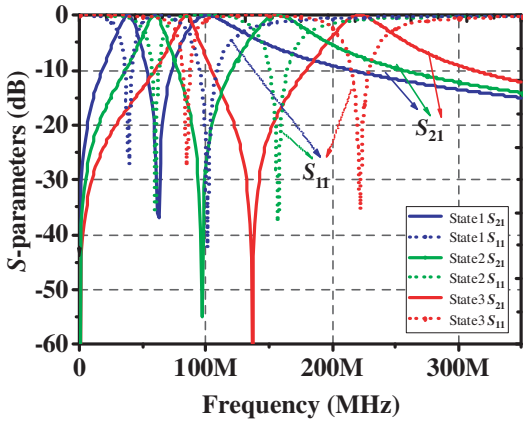

Figure 6. Simulation of a dual-band bandpass filter.

Table 1. Lumped element values for the filter at different center frequencies.

State	Centre freq.1 (MHz)	Centre freq.2 (MHz)	$L_1 = L_2$ (nH)	$C_1 = C_2$ (pF)	$Z_0(\Omega)$
State1	39	101	270	24	50
State2	60	157	270	10	50
State3	85	222	270	5	50

The actual circuit is fabricated and measured to verify the effectiveness of its performance. Considering the actual situation, the capacitor is GRM1885C1H240JA01D, and the inductor is SDCL1608CR27JTF. The values of the two devices are equal to those of the ideal situation, and the dual band-pass filter can be better realized. A photograph of the dual-band bandpass is shown in Fig. 7(a). The theoretical, simulated, and measured transmissions are compared in Fig. 7(b). As can be seen from Fig. 7(b), the centre frequency and cut-off frequency of the filter remain almost unchanged after the actual inductor and capacitor elements are chosen to replace the ideal inductor and capacitor elements, which can meet the design requirements.

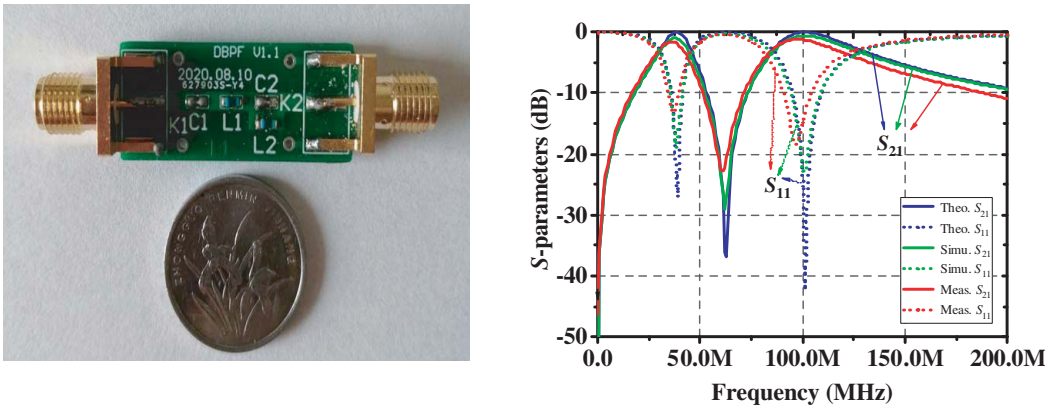

(a) (b)

Figure 7. Proposed filter: (a) The photograph of the fabricated filter; (b) Theory, simulation and measurement results.

4. REFLECTIONLESS DUAL-BAND BANDPASS FILTER

The reflection taking place in the stopband of a conventional reflective bandpass filter may cause undesired phenomena in wireless systems. These reflections back to the input can cause problems such as intermodulation interference and gain fluctuations. The absence of reflections can reduce intermodulation interference in mixers or minimize instability problems in power amplifiers without the need for additional interstage attenuators [25]. Based on the method proposed in this paper, a new reflectionless dual-band bandpass filter (RDBPF) is designed.

4.1. Design

The discharging circuit is required to implement the RDBPF. According to the circuit shown in Fig. 1, Z_2 is added in Fig. 5. The following Equations (9)–(11) are obtained. Z_2 is the impedance of the discharging circuit.

$$Z_1 = SL_1 + \frac{1}{SC_1} + \frac{1}{SC_2 + \dfrac{1}{SL_2}} \tag{9}$$

$$Z_2 = Z_0 + \frac{Z_0^2}{Z_1} = Z_0 + \frac{1}{\left(S\dfrac{L_1}{Z_0^2} + \dfrac{1}{SZ_0^2C_1}\right) + \left(\dfrac{1}{SZ_0^2C_2 + \dfrac{1}{S\dfrac{L_2}{Z_0^2}}}\right)} \tag{10}$$

$$Z_0 = R = 50\,\Omega, \quad C_3 = \frac{L_1}{Z_0^2}, \quad L_3 = Z_0^2C_1, \quad C_4 = \frac{L_2}{Z_0^2}, \quad L_4 = Z_0^2C_2 \tag{11}$$

From Equations (10) and (11), the RDBPF circuit is shown in Fig. 8. The value of each element in Z_2 can be calculated according to Equation (11).

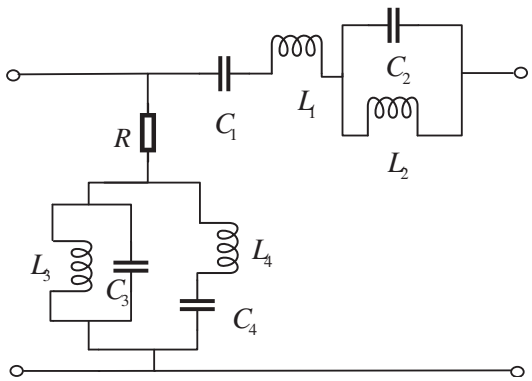

Figure 8. Reflectionless dual-band bandpass filter circuit.

The theoretical simulation results of the RDBPF are shown in Fig. 9, which achieves $S_{11} = 0 (S_{11} = -\infty\,\text{dB})$ under ideal conditions. S_{11} of the proposed filter is not shown in Fig. 9 since it is $-\infty\,\text{dB}$ over the entire frequency. The lumped element values of the RDBPF with different centre frequencies are shown in Table 2. Three different centre frequencies of RDBPF are shown. The reflection value S_{11} is not equal to zero if the capacitance and inductance are slightly changed. In practice, there is always a certain error in the capacitor and inductor, so S_{11} cannot be equal to zero.

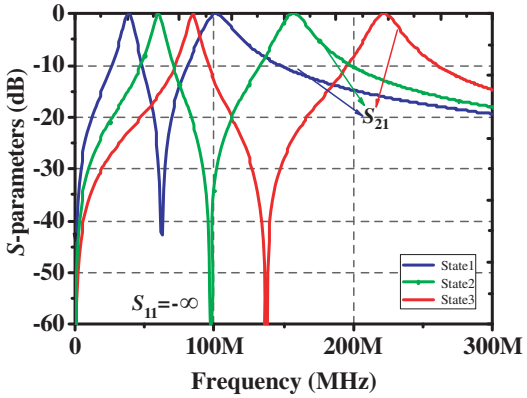

Figure 9. Theoretical simulation results of reflectionless dual-band bandpass filter.

Table 2. Lumped element values for the reflectionless filter at different centre frequencies.

State	$C_1 = C_2$ (pF)	$C_3 = C_4$ (pF)	$L_1 = L_2$ (nH)	$L_3 = L_4$ (nH)	$R(\Omega)$
State1	24	108	270	60	50
State2	10	108	270	25	50
State3	5	108	270	12.5	50

4.2. Results and Discussion

A photograph of the fabricated RDBPF is shown in Fig. 10(a). The reflection parameter S_{11} is slightly larger than the simulated one when the actual fabrication is done, as shown in Fig. 10(b). The simulation and measurement results of S_{21} are almost identical in Fig. 10(b). The insertion losses of the RDBPF are 1.9 dB and 1.4 dB at the centre frequencies 39 MHz and 101 MHz. In the rejection band frequency range, the reflection losses (S_{11}) are better than 20.6 dB and 18.1 dB for the two passbands, respectively.

The method is to add a discharging circuit to the traditional filter, rather than that the whole circuit cannot be separated as in [1] and [4]. This method is more convenient for designing a reflectionless filter and can upgrade the produced filter to have reflectionless performance, which cannot be achieved by other methods. In addition, the filter designed by this method has better performance. To illustrate the

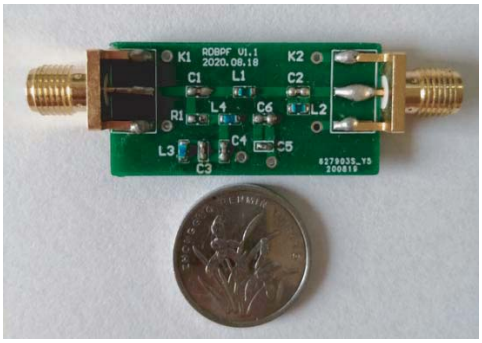

(a)

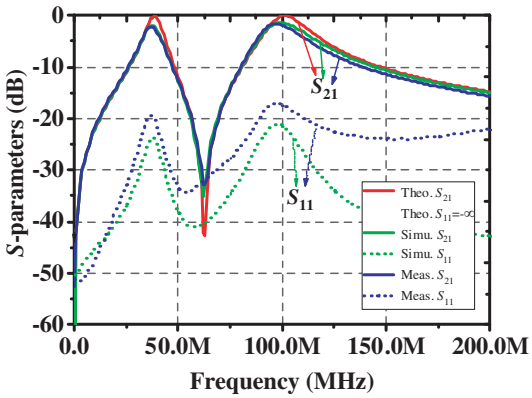

(b)

Figure 10. Proposed filter: (a) The photograph of the fabricated RDBPF; (b) Theory, simulation and measurement results of reflectionless dual-band bandpass filter.

Table 3. Comparison of microwave RDBPF and lumped parameter single pass band filter.

Parameter	[21]	[22]	[23]	[1]	This work
RL (dB)	15.1/9.3	15.9/13.6	10.1 /9.7	N/A	20.6/18.1
IL (dB)	1.9/1.7	1.47 /1.65	1.8/1.8	N/A	1.9/1.4
NE	N/A	N/A	N/A	18	11
PSR (dB)	N/A	N/A	N/A	43	51.5

RL: reflection loss, IL: insertion loss, NE: number of elements, PSR: peak stopband rejection.

advantages of the proposed RDBPF, the comparisons with the reported works are listed in Table 3. In contrast, the proposed RDBPF has higher peak stopband rejection and fewer elements than the single band bandpass filter in [1]. Compared with the microwave reflectionless dual-band bandpass filter, the proposed lumped parameter filter has a larger reflection loss in the designed frequency band, which reduces the interference to the input.

5. CASCADED FILTER AND TWO RESONANCES FILTER

When two or three reflectionless dual band-pass filters are cascaded, better frequency selectivity is realized using the cascaded filter topology, as shown in Fig. 11 and Fig. 12.

When two resonances are used, the bandwidth of the ideal reflectionless bandpass filter increases, making it more suitable for real applications. The circuit and simulation results are shown in Figs. 13(a) and (b). The values of the components are $L_1 = L_2 = 540\,\text{nH}$, $C_1 = C_2 = 12\,\text{pF}$, $L_3 = L_4 = 30\,\text{nH}$, $C_3 = C_4 = 216\,\text{pF}$.

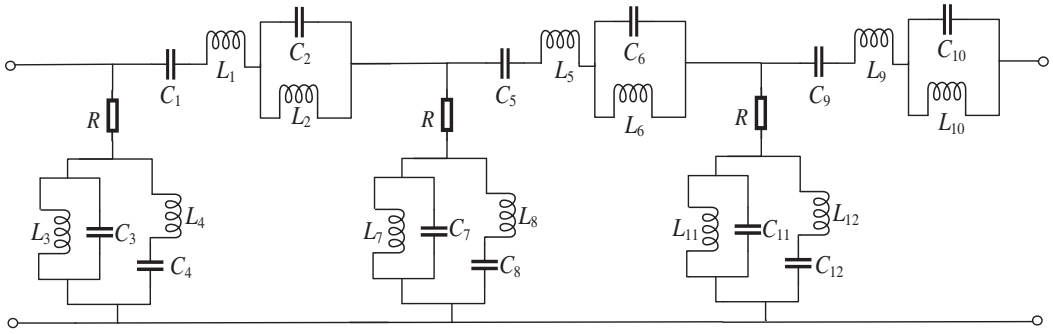

Figure 11. Cascaded reflectionless dual-band bandpass filter.

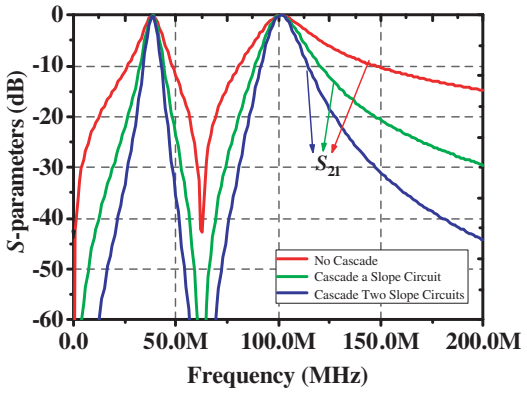

Figure 12. Theoretical simulation results of cascaded reflectionless dual-band bandpass filters.

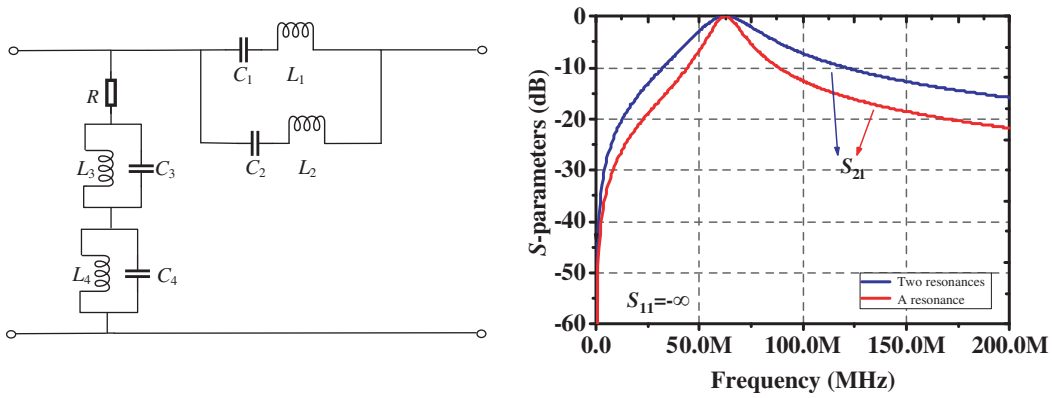

(a) (b)

Figure 13. (a) Two resonant reflectionless bandpass filter circuit. (b) Simulation of different resonant numbers.

6. CONCLUSIONS

A new design method of reflectionless filter is proposed.The reflectionless dual-band bandpass filter is implemented according to this design method. All designs are based on mathematical equation derivation. This circuit structure is simple and can be realized using available components. Simulation and measurement results of the fabricated RDBPF are almost identical. The RDBPF reduces the reflection to the input and improves the performance of the circuit.

ACKNOWLEDGMENT

This research was supported by the National Natural Science Foundation (NNSF) of China under Grant [61571075].

REFERENCES

1. Morgan, M. A. and T. A. Boyd, "Theoretical and experimental study of a new class of reflectionless filter," *IEEE Trans. Microw. Theory Techn.*, Vol. 59, No. 5, 1214–1221, 2011.
2. Morgan, M. A., *Reflectionless Filters*, 55–59, Artech House, London, 2017.
3. Morgan, M. A. and T. A. Boyd, "Reflectionless filter structures," *IEEE Trans. Microw. Theory Techn.*, Vol. 63, No. 4, 1263–1271, 2015.
4. Lee, T. H., B. Lee, and J. Lee, "First-order reflectionless lumped-element lowpass filter (LPF) and bandpass filter (BPF) design," *IMS*, 1–4, San Franciaco, CA, USA, 2016.
5. Feng, W. Y., X. K. Ma, Y. R. Shi, et al., "High-selectivity narrow- and wide-band input-reflectionless bandpass filters with intercoupled dual-behavior resonators," *IEEE Trans. Plasma Sci.*, Vol. 48, No. 2, 446–454, 2020.
6. Liu, G., M. J. Xing, X. Z. Li, et al., "Design of non-reflective bandpass filter based on IPD process," *Electron. Compon. Mater.*, Vol. 37, No. 9, 69–73, 2018.
7. Ta, H. H. and A. Pham, "Dual band band-pass filter with wide stopband on multilayer organic substrate," *IEEE Microw. Wirel. Compon. Lett.*, Vol. 23, No. 4, 193–195, 2013.
8. Park, J. H., S. J. Cheon, J. Y. Park, et al., "Compact WLAN dual-band filter using independent band stop resonators combined with diplexer," *Proc. MWS-IRFPT*, 1–2, Daejeon, 2011.
9. Li, D. and K. Xu, "Compact dual-band bandpass filter using coupled lines and shorted stubs," *Electron. Lett.*, Vol. 56, No. 14, 1721–724, 2020.

10. Mousavi, S. M. H., S. V. A. Makki, S. Alirezaee, et al., "Design of a narrow dual-band BPF with an independently tunable passband," *Electron. Lett.*, Vol. 55, No. 9, 542–543, 2019.
11. Sung, Y., "Dual-mode dual-band filter with band notch structures," *IEEE Microw. Wirel. Compon. Lett.*, Vol. 20, No. 2, 73–75, 2010.
12. Chen, X., L. Zhang, C. Xu, et al., "Dual-band filter synthesis based on two low-pass prototypes," *IEEE Microw. Wirel. Compon. Lett.*, Vol. 27, No. 10, 903–905, 2017.
13. Xu, S., F. Meng, K. Ma, K. et al., "Dual-band bandpass filter design with novel double-layer mixed coupled SIR/CPW-SIR resonators," *Proc. the IEEE MTT-S IMS*, 714–717, Boston, MA, USA, 2019.
14. Cao, P. and T. Gu, "Simple ultra-wide band band-pass filters with dual- and quad-notched bands," *Proc. ICWCSN*, 317–320, Wuhan, China, 2014.
15. Han, N., Y. Dong, and M. Wang, "A dual-band bandpass filter using parallel doubly coupled structure with loading capacitance," *Proc. ICMMT*, 1849–1851, Chengdu, China, 2010.
16. Lin, L., B. Wu, T. Su, and C. Liang , "Novel dual-band bandpass filter with wide upper stopband performance," *Xidian Univ.*, Vol. 42, No. 6, 65–70, 2015.
17. Jian, H., G. Li, H. Wang, and W. Li, "Design of a bandpass filter with independently tunable dual-band," *Shanghai Univ.*, Vol. 21, No. 2, 213–219, 2015.
18. Lalbakhsh, A., A. Ghaderi, W. Mohyuddin, et al., "A compact C-band bandpass filter with an adjustable dual-band suitable for satellite communication systems," *Electronics*, Vol. 9, No. 7, 1088, 2020.
19. Mousavi, S. H. and A. B. Kouki, "Highly compact VHF/UHF dual-band/dual-function LTCC circuits: Application to avionic systems," *IEEE T. Comp. Pack. Man*, Vol. 6, No. 1, 12–22, 2016.
20. Gómez-García, R., J. Muñoz-Ferreras, W. Feng, and D. Psychogiou, "Balanced symmetrical quasi-reflectionless singleand dual-band bandpass planar filters," *IEEE Microw. Wireless Compon. Lett.*, Vol. 28, No. 9, 798–800, 2018.
21. Cao, Z., X. Bi, Q. Xu, and H. Wu, "Compact reflectionless dual-band BPF by reused quad-mode resonator," *ComComAp*, 184–186, Shenzhen, China, 2019.
22. Gómez-García, R., J. Muñoz-Ferreras, and D. Psychogiou, "Split-type input-reflectionless multiband filters," *IEEE Microw. Wireless Compon. Lett.*, Vol. 28, No. 11, 981–983, 2018.
23. Gómez-García, R., L. Yang, J. Muñoz-Ferreras, et al., "Lossy signal-interference filters and applications," *IEEE Trans. Microw. Theory Techn.*, Vol. 68, No. 2, 516–295, 2020.
24. Gómez-García, R., L. Yang, J. Muñoz-Ferreras, et al., "Single/multi-band coupled-multi-line filtering section and its application to RF diplexers, bandpass/bandstop filters, and filtering couplers," *IEEE Trans. Microw. Theory Techn.*, Vol. 67, No. 10, 3959–3972, 2019.
25. Brooklyn, N. Y, "Reflectionless filters improve linearityand dynamic range," *Microw. J.*, Vol. 58, No. 8, 42–50, Mini-Circuits, 2015.